



HAL
open science

Short-term wave force prediction for wave energy converter control

Hoai-Nam Nguyen, Paolino Tona

► **To cite this version:**

Hoai-Nam Nguyen, Paolino Tona. Short-term wave force prediction for wave energy converter control. Control Engineering Practice, 2018, 75, pp.26-37. hal-01940727

HAL Id: hal-01940727

<https://ifp.hal.science/hal-01940727>

Submitted on 30 Nov 2018

HAL is a multi-disciplinary open access archive for the deposit and dissemination of scientific research documents, whether they are published or not. The documents may come from teaching and research institutions in France or abroad, or from public or private research centers.

L'archive ouverte pluridisciplinaire **HAL**, est destinée au dépôt et à la diffusion de documents scientifiques de niveau recherche, publiés ou non, émanant des établissements d'enseignement et de recherche français ou étrangers, des laboratoires publics ou privés.

Short-term wave force prediction for wave energy converter control

Hoi-Nam Nguyen^{*†}, Paolino Tona[†]

[†] *Control, Signal and System Department - IFP Energies Nouvelles, Rond-point de l'échangeur de Solaize BP3, 69360 Solaize, France*

hoai-nam.nguyen@ifp.fr, paolino.tona@ifp.fr

Abstract

Given the importance of wave excitation force prediction in most advanced control schemes for wave energy converters, where every new wave force estimation becomes available every fraction of second, the main objective of this paper is to perform a short-term wave prediction that can meet a trade-off between low computational complexity, limited memory usage and accuracy. To this aim, two prediction algorithms are proposed using Kalman filtering theory. The proposed prediction methods are evaluated by using real measurements.

Keywords: Wave Force Prediction, Extended Kalman Filter, Adaptive Kalman Filter, Model Predictive Control, Wave Energy Converter

1. INTRODUCTION

Wave energy converters (WECs) are devices used to produce electrical energy from wave movements. A schematic example of a WEC is given in Figure 1: an oscillating body (the captor or primary converter) moves under the action
5 of waves and is connected to a Power-Take-Off (PTO) system; the PTO, by exercising an appropriate force on the captor, converts its mechanical energy into electrical energy. The PTO can be a linear electric generator, or a multistage device, such as a hydraulic motor connected to a rotary electric generator.

^{*}Corresponding author

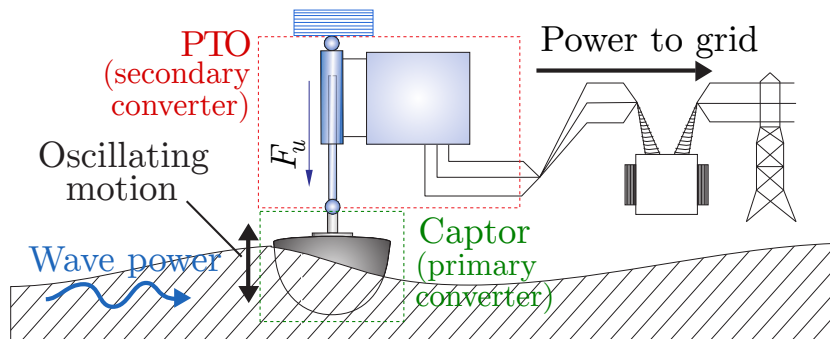


Figure 1: Schematic diagram of a wave energy converter of the point-absorber type

The PTO can be used as an actuator to adjust the natural response of the
 10 captor to waves, in order to maximize the extracted energy. The ideal conditions
 for optimal energy absorption have been studied in [1], showing that an energy
 maximizing controller requires future knowledge of the wave excitation force F_{ex} ,
 that is, the force exerted by the incoming wave on the captor. Among the many
 different approaches to hydrodynamic control of WECs, see [2] for a thorough
 15 review, latching control [3], [4], declutching control [5], and model predictive
 control (MPC) [6] are examples of strategies relying, directly or indirectly, on
 this knowledge. In the MPC context, for instance, the complete control scheme
 must include an online algorithm to compute future values of the wave excitation
 force over the prediction horizon, as shown in Figure 2.

20 Notice that, while it is relatively straightforward to measure excitation force
 using a dedicated experiment and a well-positioned force sensor [7], only indi-
 rect measurements or estimations are possible during normal WEC operation.
 Two experimentally-validated methods for wave force estimation from available
 measurements are described in [7]. Assuming that local wave elevation mea-
 25 surements are possible during WEC operation, another, less direct, approach
 could consist of computing future values of the wave excitation force from wave
 elevation predictions, though this would require an inconvenient increase of the
 prediction horizon, to cope with the non-causal nature of the impulse function

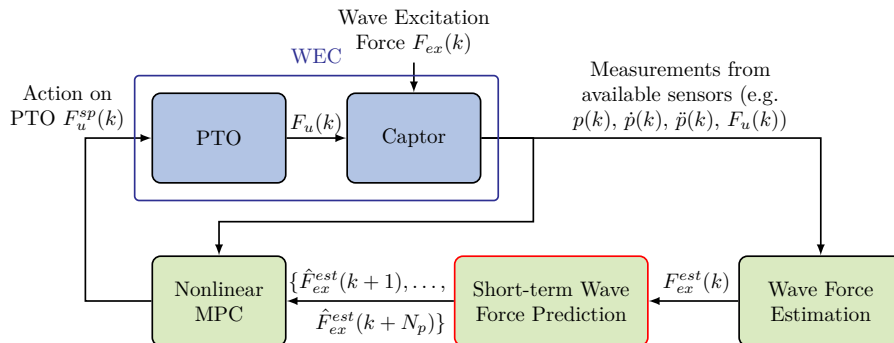


Figure 2: Wave excitation force prediction in the context of MPC

relating wave elevation to wave excitation force. Indeed, for its important role
 30 in the optimization of WEC energy yield, short-term wave forecasting, with a
 particular focus on wave elevation, has drawn a lot of attention in the hydrody-
 namic control community.

A first possible approach to perform short-term wave forecasting is spatial
 prediction, using up-wave measurements from sensors installed around the loca-
 35 tion of a WEC [8], [9], [10]. The method is reported to forecast quite long pre-
 diction horizons with a good performance [11]. However the forecasting model
 can become very complex, since the wave propagation nonlinearities or/and the
 possible multi-directionality of waves have to be taken into account [12].

A second approach, that has become popular in the last years because of
 40 its simplicity, is to use past time series of local measurements or estimates, at
 the float position. In [13], using real wave elevation data, Fusco and Ringwood
 show that a relatively simple linear auto-regressive (AR) model can perform
 quite well, provided that the high-frequency content is filtered out from the time
 series data. To avoid introducing a phase lag, the use of a non-causal zero-phase
 45 filter is advocated. The solution is based on a *batch-processing* approach, which
 also includes a computationally-expensive nonlinear least squares problem to be
 solved and a spectral analysis to be performed in order to compute an optimal
 sampling period for all the computations. It is worth noticing that considering

a more complex model structure in this context, namely an auto regressive
50 moving average (ARMA) model instead of an AR model, does not seem to
bring any particular benefit [14]. In [15], an iterative, more easily implementable
approach is proposed, based on a bank of least squares estimators. However,
as it will be shown later, it is implicitly assumed that the sea state is constant.
Furthermore, as noticed in [15], the prediction performance degrades as quickly
55 as the prediction horizon increases.

Two novel solutions for short-term wave forecasting are proposed in this
paper. They are also based on past time series of local WEC measurements
or estimates. Implementation aspects such as computational complexity and
accuracy are investigated. Their performance is assessed using wave excitation
60 force time series, obtained from data collected in the wave basin of Aalborg
University, on a lab-scale wave energy converter prototype.

Three main features of the proposed solutions, built around AR-model esti-
mation, are:

- It is shown that, for the first method, the multi-step ahead error criterion
65 adopted in [13] is a particular case of our criterion.
- The first method is based on the extended Kalman filter. Hence the
algorithm is recursive and easy to implement.
- To improve the performance, overcoming the error accumulation problem
that comes with the first method, an alternative approach is proposed. It
70 builds an independent model for each horizon, using an adaptive Kalman
filter. It is also shown that the approach in [15] is a limiting case of ours,
when the sea state is assumed to be constant.

The paper is organized as follows. The problem is formulated in Section 2
together with a review from the literature. Then the multi-step error minimiza-
75 tion approach with extended Kalman filter is proposed in Section 3, while in
Section 4, an adaptive Kalman filtering approach is considered. In Section 5,
the available data as well as the prediction results are presented. In Section 6

the computation of a forecasting interval is considered. Some conclusions are drawn in Section 7.

80 2. PROBLEM FORMULATION

Given available estimates $\{\hat{F}_{ex}(l)\}$ of the wave excitation force taken at discrete time instants $l = 0, 1, \dots, k$, where k is the current time, our objective is to predict the wave excitation force at time $k + 1, k + 2, \dots, k + N_p$, where N_p is the prediction horizon. For this purpose, some prediction methods in the literature are first reviewed. These methods will be compared to the new approaches developed in the paper. In the following, for simplicity denote $y(k) = \hat{F}_{ex}(k)$.

2.1. Decomposition based approach

This approach is based on the assumption that $y(k)$ may be regarded as the sum of several sinusoidal waves of different frequencies, amplitudes and phases,

$$y(k) = \sum_{j=1}^m A_j \sin(\omega_j k + \phi_j) \quad (1)$$

where m is the total number of components, A_j , ω_j and ϕ_j are the amplitude, the angular wave frequency and the phase angle of the j th component, respectively [16]. Note that in the model (1) the frequencies ω_j are known and fixed, while A_j and ϕ_j are unknown. The parameters A_j and ϕ_j can be estimated through least squares or Kalman filter procedures and can be used to forecast the future wave excitation force [13].

The main advantage of the model (1) is its direct physical meaning. However the constant frequencies assumption is rather restrictive and unrealistic, since it is well known that the wave excitation force spectrum is time-varying [17]. Consequently, it is not reliable to use the model (1) to predict the future wave excitation force.

2.2. Sinusoidal extrapolation based approach

The idea is to model $y(k)$ as a single sinusoidal signal with a time-varying frequency, amplitude and phase,

$$y(k) = A(k)\sin(\omega(k)k + \phi(k)) \quad (2)$$

105 where $A(k)$, $\omega(k)$ and $\phi(k)$ are unknown.

Evidently, the model (2) is nonlinear in $A(k)$, $\omega(k)$ and $\phi(k)$. As a consequence, a linear recursive estimator cannot be directly applied. It is possible, however, to use a truncated Taylor expansion of (2), and then an extended Kalman filter (EKF) to estimate the values of $A(k)$, $\omega(k)$ and $\phi(k)$ [13].

110 A direct physical meaning is also an advantage of model (2). However, it is clear that using one sinusoid to describe a wave is only effective for very narrow-banded wave systems. In addition, the extension to a model with multiple time-varying frequencies is not as straightforward as it may seem.

2.3. Auto-regressive model based approach

115 The AR model is based on the assumption that $y(k)$ at time k is a linear function of its past observations $y(k-1), y(k-2), \dots, y(k-p)$, i.e.

$$y(k) = a_1y(k-1) + a_2y(k-2) + \dots + a_py(k-p) + w(k) \quad (3)$$

where (a_1, a_2, \dots, a_p) are the parameters, p is the order of the model, and $w(k)$ is a zero-mean white noise disturbance.

Assume that, at time k , the coefficients $a_j, \forall j = 1, 2, \dots, p$ are already
 120 calculated. Note that $a_j, \forall j = 1, 2, \dots, p$ might be time-varying, i.e. $a_j = a_j(k)$ might also be functions of time. It is well known [18] that the best prediction of $\hat{y}(k+h|k)$ at time k can be calculated as,

$$\hat{y}(k+h|k) = a_1(k)\hat{y}(k+h-1|k) + a_2(k)\hat{y}(k+h-2|k) + \dots + a_p(k)\hat{y}(k+h-p|k) \quad (4)$$

where $\hat{y}(k+h-j|k) = y(k+h-j)$ if $k+h-j \leq k$ or equivalently, if $h-j \leq 0$. It is shown in [13] that the AR model (3) with only complex-conjugate

125 poles is equivalent to model (1), where the angular frequencies are calculated automatically.

Rewrite (3) in a compact vector form as

$$y(k) = x_{ar}(k-1)^T \mathbf{a} + w(k) \quad (5)$$

where

$$\begin{cases} x_{ar}(k-1) = [y(k-1) & y(k-2) & \dots & y(k-p)]^T, \\ \mathbf{a} = [a_1 & a_2 & \dots & a_p]^T \end{cases}$$

The simplest way to estimate a_j , $j = 1, 2, \dots, p$ at time k , consists of minimizing
 130 the one-step ahead prediction error which results in a least squares problem,

$$\min_{a_1, a_2, \dots, a_p} \sum_{l=p+1}^k (y(l) - \hat{y}(l|l-1))^2 \quad (6)$$

It is well known [19] that the optimal solution \mathbf{a}^* to (6) can be obtained analytically.

Theoretically, if the model structure (3) exactly matches the structure of the actual system, and the signal to noise ratio is high, then the model obtained
 135 using (6) is the best linear unbiased estimator, which also provides optimal multi-step ahead predictions. However, Fourier analysis reveals that real wave excitation force estimates are generally quite noisy. In addition, it is not possible to know the exact model structure of the real system to be identified. Consequently, it is not reliable to use the cost function (6) to produce accurate
 140 predictions over an entire forecasting horizon.

One way to improve the accuracy given by model (3) in forecasting is to consider the multi-step ahead error minimization, referred to as *long-range predictive identification* (LRPI) [20], [13],

$$\min_{a_1, a_2, \dots, a_p} \sum_{l=p+M+1}^k \sum_{j=1}^M (y(l) - \hat{y}(l|l-j))^2 \quad (7)$$

where M is the forecasting horizon over which the AR model is to be optimized.
 145 Parameters estimated from objective functions based on multi-step ahead predictors, generally result in better models for wave forecasting. In addition to

the time domain interpretation, Wahlberg and Ljung [21] showed that the use of multi-step ahead error minimization method amounts to emphasizing the accuracy of low-frequency dynamics more in distributing the bias, compared to
 150 the one-step-ahead error minimization, which tends to put higher emphasis on the high frequency behavior.

Unfortunately, the optimization problem based on the multi-step ahead error minimization criterion (7) is nonlinear. Hence, in general, no analytical solution a_j^* can be found. One may, however, use the Gauss-Newton algorithm to obtain
 155 a local optimal solution as indicated in [13].

3. EXTENDED KALMAN FILTERING APPROACH

The Gauss-Newton based solution in Section 2.3 is a *batch - processing* approach and in a non-recursive form, which might be difficult to realize in practice. The solution is ill-adapted for on-line identification because of its computational and storage costs. In addition, until a new optimal solution a_j^* is found,
 160 it is implicitly assumed that the coefficients a_j^* are constant. This assumption, as it will be shown later, is rather restrictive.

The main contribution of this section is to propose a new algorithm for the multi-step ahead error minimization method. The approach is based on the EKF
 165 procedure, and hence is recursive. To the best of the authors' knowledge, this is the first time that the EKF is applied to the multi-step ahead error minimization method. The sea state time-varying nature is handled via a process noise in the state equation, as it will be shown in the next section.

3.1. State space equation for the filter

170 Since the sea state varies with time, but the variation is slow, it can be assumed that, $\forall j = 1, 2, \dots, p$,

$$a_j(k+1) = a_j(k) + \eta_j(k) \tag{8}$$

where $\eta_j(k)$ is used to describe the variation of $a_j(k)$.

Remark 1: It is worth noticing that allowing $a_j(k)$ to be time-varying is also a way to compensate the fact that the AR model (3) is only an approximation
 175 of the real wave excitation force model.

Equation (8) can be rewritten in a compact vector form as,

$$\mathbf{a}(k+1) = \mathbf{a}(k) + \boldsymbol{\eta}(k) \quad (9)$$

where

$$\begin{cases} \mathbf{a}(k) = [a_1(k) \ a_2(k) \ \dots \ a_p(k)]^T, \\ \boldsymbol{\eta}(k) = [\eta_1(k) \ \eta_2(k) \ \dots \ \eta_p(k)]^T \end{cases}$$

At time k , for the multi-step ahead error minimization method, one would like to have:

- 180 • A small one-step ahead prediction error

$$\epsilon_1(k) = y(k) - \hat{y}(k|k-1) \quad (10)$$

where

$$\hat{y}(k|k-1) = x_{ar}(k-1)^T \mathbf{a}(k).$$

- A small two-step ahead prediction error

$$\epsilon_2(k) = y(k) - \hat{y}(k|k-2) \quad (11)$$

where $\hat{y}(k|k-2)$ is the wave prediction at time k using $y(k-2), y(k-3), \dots$. The value of $\hat{y}(k|k-2)$ can be calculated iteratively via $\hat{y}(k-1|k-2)$ as

$$\hat{y}(k|k-2) = a_1(k)\hat{y}(k-1|k-2) + a_2(k)y(k-2) + \dots + a_p(k)y(k-p)$$

185 where

$$\hat{y}(k-1|k-2) = a_1(k)y(k-2) + a_2(k)y(k-3) + \dots + a_p(k)y(k-p-1)$$

Hence

$$\begin{aligned} \hat{y}(k|k-2) &= (a_1(k)^2 + a_2(k))y(k-2) + (a_1(k)a_2(k) + a_3(k))y(k-3) \\ &\quad + \dots + a_1(k)a_p(k)y(k-p-1) \end{aligned} \quad (12)$$

- A small l -step ahead prediction error, $\forall l = 3, 4, \dots, M$

$$\epsilon_l(k) = y(k) - \hat{y}(k|k-l) \quad (13)$$

where $\hat{y}(k|k-l)$ is the prediction at time k using $y(k-l), y(k-l-1), \dots$

The value of $\hat{y}(k|k-l)$ can be calculated in a similar way as for $\hat{y}(k|k-2)$.

190 Recall that M is the forecasting horizon over which the AR model is to be optimized.

Combining (10), (11), (13), one obtains,

$$\left\{ \begin{array}{l} y(k) = \hat{y}(k|k-1) + \epsilon_1(k), \\ y(k) = \hat{y}(k|k-2) + \epsilon_2(k), \\ \vdots \\ y(k) = \hat{y}(k|k-M) + \epsilon_M(k) \end{array} \right. \quad (14)$$

Equation (14) is considered as an output equation for the EKF. The residuals

$\epsilon_j(k)$, $\forall j = 1, 2, \dots, M$ are assumed to be a noise, which also represents the

195 measurement disturbance.

Together with (8), one gets the following state space equation,

$$\left\{ \begin{array}{l} \mathbf{a}(k+1) = \mathbf{a}(k) + \eta(k), \\ \left[\begin{array}{c} y(k) \\ y(k) \\ \vdots \\ y(k) \end{array} \right] = \left[\begin{array}{c} \hat{y}(k|k-1) \\ \hat{y}(k|k-2) \\ \vdots \\ \hat{y}(k|k-M) \end{array} \right] + \epsilon(k) \end{array} \right. \quad (15)$$

where $\epsilon(k) = [\epsilon_1(k) \ \epsilon_2(k) \ \dots \ \epsilon_M(k)]^T$.

The state equation of (15) is linear with respect to (w.r.t) the *state* or the parameters a_j , $j = 1, 2, \dots, p$. However, using (12), it is clear that the output

200 equation of (15) is nonlinear w.r.t. a_j . In this paper, to estimate $\mathbf{a}(k)$, the EKF method is applied due to its simplicity, optimality, tractability and robustness.

3.2. Extended Kalman filter

In essence, for system (15), the EKF filter provides a solution to the following minimization problem

$$\min_{\mathbf{a}(k)} J_a(k) \quad (16)$$

with a cost function defined as

$$J_a(k) = (\mathbf{a}(0) - \mathbf{a}(0|0))^T P_0^{-1} (\mathbf{a}(0) - \mathbf{a}(0|0)) + \sum_{l=1}^k (\eta(l-1)^T Q^{-1} \eta(l-1) + \epsilon(l)^T R^{-1} \epsilon(l)) \quad (17)$$

where $\mathbf{a}(0|0)$ is the mean value of $\mathbf{a}(0)$, P_0, Q, R are weighting matrices. Recall that $\eta(k) = \mathbf{a}(k+1) - \mathbf{a}(k)$, and

$$\epsilon(k) = \begin{bmatrix} y(k) \\ y(k) \\ \vdots \\ y(k) \end{bmatrix} - \begin{bmatrix} \hat{y}(k|k-1) \\ \hat{y}(k|k-2) \\ \vdots \\ \hat{y}(k|k-M) \end{bmatrix}$$

Consider the following limiting case, where

- No information about initial state $\mathbf{a}(0)$ is available. Then one should choose a large P_0 . Therefore $(\mathbf{a}(0) - \mathbf{a}(0|0))^T P_0^{-1} (\mathbf{a}(0) - \mathbf{a}(0|0))$ can be neglected in the objective function (17).
- The sea state is time-invariant. Hence, $\forall k$,

$$\mathbf{a}(k+1) = \mathbf{a}(k)$$

and $\eta(k) = 0$.

In this case, the cost function (17) can be rewritten as,

$$J_a(k) = \min_{\mathbf{a}} \sum_{l=1}^k \epsilon(l)^T R^{-1} \epsilon(l)$$

If R is the identity matrix, and by re-indexing l , one obtains

$$J_a(k) = \min_{\mathbf{a}} \sum_{l=p+M+1}^k \sum_{j=1}^M (y(l) - \hat{y}(l|l-j))^2$$

Thus one obtains the cost function (7) of LRPI. Hence (7) is a particular case of (17), when the sea state is time invariant and the initial parameter $\mathbf{a}(0)$ is completely unknown.

Remark 2: Note that the multi-step ahead error minimization cost (7) can be used to obtain information about $\mathbf{a}(0)$. However, a solution of a nonlinear least squares problems is required. In this work, the matrix P_0 has been set large. This implies no information about $\mathbf{a}(0)$ is available.

Remark 3: Recall that an estimator [7] is used to estimate the wave excitation force $y(k)$ in this work. Consequently, the measurement noise matrix R for the EKF is known. There are several methods in the literature to estimate the process noise matrix Q such as maximum like-hood estimation [22], correlation method [23], [24], etc. However due to the limited time available for the tests, the trial and error method is used to tune Q . The basic idea is to first try to find the main diagonal, and then the first and the second sub-diagonal elements of Q . The other sub-diagonal elements of Q are set to be zero in this work.

The following notations are adopted,

- $\hat{\mathbf{a}}(k|k-1)$ is the estimate of $\mathbf{a}(k)$ given measurements from time $k-1$, i.e. $y(k-1), y(k-2), \dots$,
- $\hat{\mathbf{a}}(k|k)$ is the estimate of $\mathbf{a}(k)$ given measurements from time k , i.e. $y(k), y(k-1), \dots$,
- $P(k|k-1)$ is the covariance matrix of $\mathbf{a}(k)$ given $y(k-1), y(k-2), \dots$,
- $P(k|k)$ is the covariance matrix of $\mathbf{a}(k)$ given $y(k), y(k-1), \dots$,

Then the EKF procedure is summarized as follows,

- Time update,

$$\begin{cases} \hat{\mathbf{a}}(k|k-1) &= \hat{\mathbf{a}}(k-1|k-1), \\ P(k|k-1) &= P(k-1|k-1) + Q \end{cases} \quad (18)$$

- Measurement update,

$$\left\{ \begin{array}{l} K(k) = P(k|k-1)H(k) (H(k)^T P(k|k-1)H(k) + R)^{-1} \\ \hat{\mathbf{a}}(k|k) = \hat{\mathbf{a}}(k|k-1) + K(k) \left(\begin{bmatrix} y(k) \\ y(k) \\ \vdots \\ y(k) \end{bmatrix} - \begin{bmatrix} \hat{y}(k|k-1) \\ \hat{y}(k|k-2) \\ \vdots \\ \hat{y}(k|k-M) \end{bmatrix} \right) \\ P(k|k) = (I - K(k)H(k)) P(k|k-1) \end{array} \right. , \quad (19)$$

with

$$H(k) = \left. \frac{dh(k)}{d\mathbf{a}} \right|_{\mathbf{a}=\hat{\mathbf{a}}(k|k-1)} \quad (20)$$

where I is the identity matrix of appropriate dimension, and

$$h(k) = \begin{bmatrix} \hat{y}(k|k-1) \\ \hat{y}(k|k-2) \\ \vdots \\ \hat{y}(k|k-M) \end{bmatrix}$$

Once the optimal parameter $\hat{\mathbf{a}}(k|k)$ is found, it can be used to forecast the wave excitation force as follows,

Algorithm 1: Wave force forecasting based on parameters estimated by the EKF filter

1. **Input:** Wave estimates $y(k), y(k-1), \dots$, Estimated parameters $\hat{\mathbf{a}}(k|k)$, Forecasting horizon N_p
 2. **Output:** $\hat{y}(k+1|k), \hat{y}(k+2|k), \dots, \hat{y}(k+N_p|k)$
- (i) Initialization $s = 1$ and

$$x = [y(k) \ y(k-1) \ \dots \ y(k-p+1)]^T$$

(ii) Calculate the predictions $\hat{y}(k + s|k)$ as,

$$\begin{cases} y_f = x^T \hat{\mathbf{a}}(k|k), \\ \hat{y}(k + s|k) = y_f, \\ x = [y_f \ x(1 : p - 1)^T]^T, \\ s = s + 1 \end{cases}$$

(iii) If $s \leq N_p$, then go to Step (ii), otherwise Stop.

Algorithm 1 is schematically presented in Figure 3. It is worth noticing that $\hat{y}(k + j|k)$ is used to predict $\hat{y}(k + j + 1|k)$. Hence Algorithm 1 can be classified as an *iterative* procedure. Since only one model is required, significant computational time can be saved, especially when the forecast horizon is large.

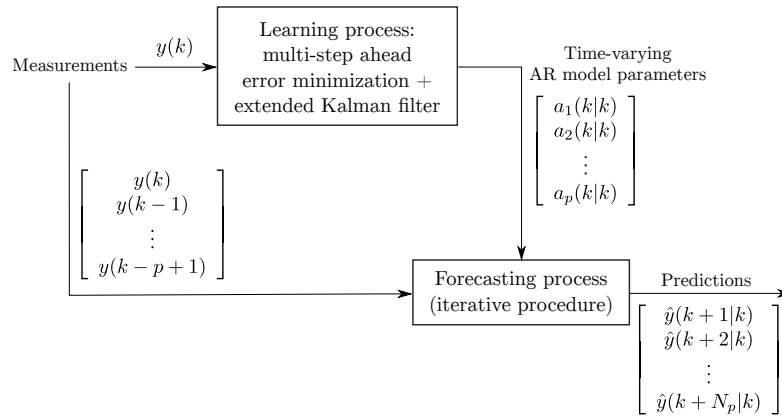


Figure 3: Synoptic of the wave excitation force prediction method using EKF filter.

4. ADAPTIVE KALMAN FILTERING APPROACH

As discussed in Section 3, low computational complexity is the main advantage of algorithm 1. However, since the predicted values from the past are used to predict the future, it can be shown that the approach suffers from an error

accumulation problem, i.e. errors committed in the past are propagated into future predictions.

For the short-term wave excitation force forecasting, an alternative approach, that does not suffer from the error accumulation problem, is proposed in this Section. The main idea is to use an *optimal* h -step ahead prediction model for each $h = 1, 2, \dots, N_p$, where N_p is the prediction horizon. Then all the N_p models are simultaneously used for predictions.

The new method is based on the assumption that the wave excitation force $y(k+h)$ at time $k+h$ is a linear function of its past estimates $y(k), y(k-1), \dots, y(k-p+1)$, i.e.

$$y(k+h) = \sum_{j=1}^p a_{j,h}(k)y(k-j+1) + \epsilon(k+h) \quad (21)$$

where $h = 1, 2, \dots, N_p$ is the forecasting horizon, p is the order of the model. Note that p can be different for different h . $\epsilon(k+h)$ is a zero mean white noise. $\mathbf{a}_h(k) = [a_{1,h}(k) \ a_{2,h}(k) \ \dots \ a_{p,h}(k)]^T$ are the parameters to be estimate.

At time k , it is well known [18] that the best prediction of the future wave excitation force $\hat{y}(k+h|k)$ is

$$\hat{y}(k+h|k) = \sum_{j=1}^p a_{j,h}(k)y(k-j+1) \quad (22)$$

Clearly, $\mathbf{a}_h(k)$ need to be estimated in order to forecast $\hat{y}(k+h|k)$. One of the most common ways to do this is to assume that

$$\mathbf{a}_h(k+1) = \mathbf{a}_h(k) \quad (23)$$

and then to solve the following least squares optimization problem [15]

$$\min_{\mathbf{a}_h} \sum_{l=p+h+1}^k (y(l) - \hat{y}(l|l-h))^2 \quad (24)$$

which one will refer to as *multi-model long range prediction identification* (MM-LRPI), or multi-model multi-step ahead error minimization. It is well known [15], [25] that the solution to (24) can be found analytically using the least squares method.

It is worth noticing that equation (23) does not take into account the sea state time-varying nature. A more realistic solution to find $\mathbf{a}_h(k)$, is to use the weighted least squares method, resulting in the following cost function,

$$\min_{\mathbf{a}_h} \sum_{l=p+h+1}^k \lambda^{k-l} (y(l) - \hat{y}(l|l-h))^2 \quad (25)$$

where $\lambda \in (0, 1]$ is the forgetting factor. However, it is well known [26] that, when the measurements do not give any new information to the system, one might have the *blow-up* phenomenon with the weighted least squares method.

Below a way to estimate $\mathbf{a}_h(k)$ is provided, for which the time-varying nature of sea state is taken into account. For this purpose, rewrite (21) as,

$$y(k) = \sum_{j=1}^p a_{j,h}(k-h) y(k-h-j+1) + \epsilon(k) \quad (26)$$

Since the sea state is time-varying, but the variation is slow, it can be assumed that, $\forall j = 1, 2, \dots, p$,

$$a_{j,h}(k+1) = a_{j,h}(k) + \eta_j(k) \quad (27)$$

where $\eta_j(k)$, $\forall j = 1, 2, \dots, p$, are the noises. Denote

$$\eta(k) = [\eta_1(k) \ \eta_2(k) \ \dots \ \eta_p(k)]^T$$

Using (27), one has,

$$\begin{aligned} \mathbf{a}_h(k) &= \mathbf{a}_h(k-1) + \eta(k-1) \\ &= \mathbf{a}_h(k-2) + \eta(k-2) + \eta(k-1) \\ &= \dots \\ &= \mathbf{a}_h(k-h) + \sum_{v=1}^h \eta(k-v) \end{aligned}$$

Hence

$$\mathbf{a}_h(k-h) = \mathbf{a}_h(k) - \sum_{v=1}^h \eta(k-v) \quad (28)$$

Equation (26) can be rewritten as

$$y(k) = x_h(k)^T \mathbf{a}_h(k) + \mu(k) \quad (29)$$

where

$$\begin{cases} x_h(k) = [y(k-h) \ y(k-h-1) \ \dots \ y(k-h-p+1)]^T, \\ \mu(k) = -x_h(k)^T \sum_{v=1}^h \eta(k-v) + \epsilon(k) \end{cases}$$

Combining (27), (29), the following state space equation is obtained

$$\begin{cases} \mathbf{a}_h(k+1) &= \mathbf{a}_h(k) + \eta(k), \\ y(k) &= \sum_{j=1}^p a_{j,h}(k)y(k-h-j+1) + \mu(k) \end{cases} \quad (30)$$

300 Evidently, $\mathbf{a}_h(k)$ enters linearly in equation (30). One way to estimate optimally and recursively the unknown *state* vector $\mathbf{a}_h(k)$ is to apply the linear Kalman filter (LKF) algorithm [27]. In essence, the LKF provides the solution of the optimization problem

$$\min_{\mathbf{a}_h(k)} J_a(k)$$

with

$$\begin{aligned} J_a(k) &= (\mathbf{a}_h(0) - \mathbf{a}_h(0|0))^T P_0^{-1} (\mathbf{a}_h(0) - \mathbf{a}_h(0|0)) + \\ &\quad + \sum_{l=1}^k (\eta(l-1)^T Q_h^{-1} \eta(l-1) + \mu(l)^T R_h^{-1} \mu(l)) \end{aligned} \quad (31)$$

305 where P_0, Q_h, R_h are weighting matrices, $\mathbf{a}_h(0|0)$ is the mean value of the initial state $\mathbf{a}_h(0|0)$. Recall that

$$\begin{cases} \eta(k) = \mathbf{a}_h(k+1) - \mathbf{a}_h(k) \\ \mu(k) = y(k) - \sum_{j=1}^p a_{j,h}(k)y(k-h-j+1) \end{cases}$$

Consider now the following limit case, where

- No information about initial state $\mathbf{a}(0)$ is available. Hence P_0 should be chosen very large. As a consequence $(\mathbf{a}_h(0) - \mathbf{a}_h(0|0))^T P_0^{-1} (\mathbf{a}_h(0) - \mathbf{a}_h(0|0))$ is a negligible term in the cost function (31).
- The sea state is time-invariant. Hence, $\forall k$,

$$\mathbf{a}(k+1) = \mathbf{a}(k)$$

and $\eta(k) = 0$.

In this case, the cost function (31) can be rewritten as,

$$J_a(k) = \min_{\mathbf{a}} \sum_{l=1}^k \mu(l)^T R_h^{-1} \mu(l)$$

If R_h is the identity matrix, and by re-indexing l , one obtains

$$J_a(k) = \min_{\mathbf{a}_h} \sum_{l=p+h+1}^l (y(l) - \hat{y}(l|l-h))^2$$

315 Thus the cost function (24) of MM-LRPI is obtained. Hence (24) is a particular case of (27), when the sea state is time invariant and the initial parameter $\mathbf{a}(0)$ is completely unknown.

Remark 4: With the appropriate choice of forgetting factor, the method in [15] can also cope with a time-varying sea state. However, beside the fact 320 that the weighted least squares method might lead to the *blow-up* phenomenon, the Kalman filter based method has more tuning parameters, i.e., more degrees of freedom than the weighted least squares method. Hence the Kalman filter based method is a better choice than the weighted least squares based method.

Using the same notation as in Section 3 for $\hat{\mathbf{a}}_h(k|k-1)$, $\hat{\mathbf{a}}_h(k|k)$, $P_h(k|k-1)$ 325 and $P_h(k|k)$, the LKF algorithm is summarized as follows

- Time update

$$\begin{cases} \hat{\mathbf{a}}_h(k|k-1) &= \hat{\mathbf{a}}_h(k-1|k-1), \\ P_h(k|k-1) &= P_h(k-1|k-1) + Q_h \end{cases} \quad (32)$$

- Measurement update

$$\begin{cases} K_h(k) &= P_h(k|k-1)x_h(k) (x_h(k)^T P_h(k|k-1)x_h(k) + R_h)^{-1} \\ \hat{\mathbf{a}}_h(k|k) &= \hat{\mathbf{a}}_h(k|k-1) + K(k) (y(k) - x_h(k)^T \hat{\mathbf{a}}_h(k|k-1)), \\ P_h(k|k) &= (I - K(k)x_h(k)) P_h(k|k-1) \end{cases} \quad (33)$$

where

$$x_h(k) = [y(k-h) \ y(k-h-1) \ \dots \ y(k-h-p+1)]^T, \quad (34)$$

Once the optimal parameter $\mathbf{a}_h(k|k)$ is calculated, it can be used in producing 330 the forecasting horizon $\hat{y}(k+h|k)$ as follows

Algorithm 2: Wave force forecasting based on parameters estimated by the AKF filters

1. **Input:** Wave estimates $y(k), y(k-1), \dots$, Prediction horizon N_p , Covariance matrices Q_h, R_h , Estimations $\hat{\mathbf{a}}_h(k-1|k-1), P_h(k-1, k-1), \forall h = 1, 2, \dots, N_p$

335

2. **Output:** Prediction $\hat{y}(k+h|k), \forall h = 1, 2, \dots, N_p$
- (i) Initialization: $h = 1$
 - (ii) Calculate the vector,

$$x_{ar}(k) = \begin{bmatrix} y(k) & y(k-1) & \dots & y(k-p+1) \end{bmatrix}^T$$

- (iii) Apply the LKF (32), (33), (34) to obtain $\hat{\mathbf{a}}_h(k|k), P_h(k, k)$

340

- (iv) The prediction $\hat{y}(k+h|k)$ is computed as,

$$\hat{y}(k+h|k) = x_{ar}(k)^T \hat{\mathbf{a}}_h(k|k)$$

- (v) Set $h := h + 1$
- (vi) If $h \leq N_p$, then go to Step (iii). Otherwise Stop.

Algorithm 2 is schematically presented in Figure 4. Note that N_p linear Kalman filters are used to obtain $\hat{y}(k+1|k), \hat{y}(k+2|k), \dots, \hat{y}(k+N_p|k)$. Consequently, this approach involves a heavier computational burden than iterative forecasting.

345

5. EXPERIMENTAL RESULTS

5.1. Available data

The wave data utilized for this study were collected in a wave basin of Aalborg University (15 m long, 8 m wide and 0.7 m deep), in the context of an experimental assessment of the performance of a nonlinear MPC strategy applied to a WEC prototype [28].

350

The WEC under consideration (shown in Figure 5) is a 1 : 20 scale laboratory prototype of the well-known Wavestar machine installed near Hanstholm

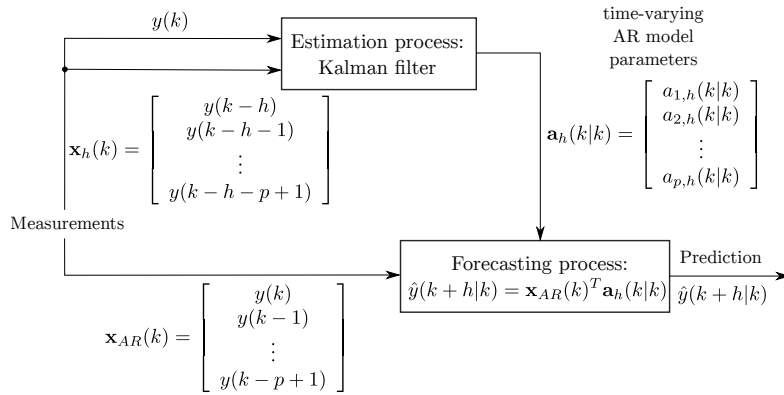


Figure 4: Synoptic of the wave excitation force prediction method using AKF filter.

355 in Denmark from 2009 to 2013. It consists of a nearly hemispherical float, mechanically hinged to a fixed reference point (only one of the five available floats was used for the experiments).

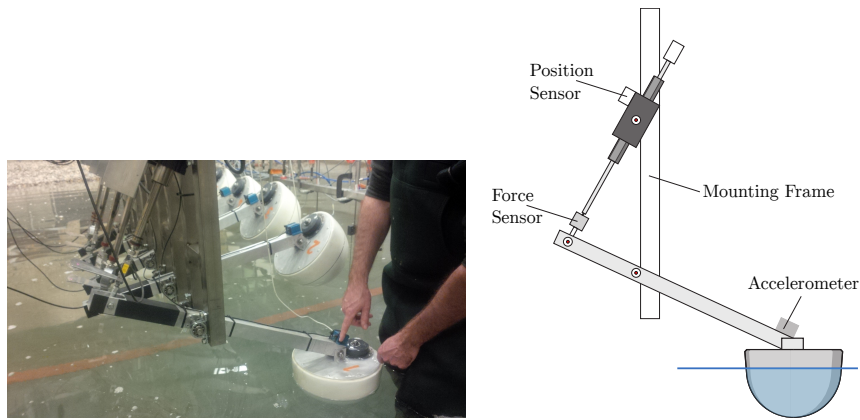


Figure 5: Experimental set-up at the wave basin of Aalborg University

A linear motor is used to emulate the action of the PTO. An accelerometer and a position sensor provide measurements of the float motion, while a load cell
 360 provides a measurement of the force applied by the linear motor. A rapid control prototyping architecture, based on the Matlab xPCTarget toolbox, allows to run controllers developed in Simulink in real-time (up to 1 kHz) on a target PC

connected to the WEC I/O board. In Simulink, all the linear measurements are transparently converted into the angular reference frame corresponding to the single degree of freedom of the WEC (rotation around the hinge point). Float
 365 angular velocity is estimated from acceleration and position, using a Kalman filter.

The MPC controller validated in the experimental campaign has the structure represented in Figure 2, except that position, velocity and acceleration are
 370 angular, and moments replace forces.

The data considered for the present analysis are time series of wave moment estimates (the output of the “Wave Force Estimation” block in Figure 2), logged during closed-loop experiments where MPC is used to maximize WEC electric energy production, under the action of different irregular waves. A set
 375 of four different irregular waves, each generated from a different wave spectrum, is considered. The spectra are representative of the most common sea state conditions in Hanstholm, adapted in scale to the WEC prototype in the basin, via the Froude similarity laws (see Table 1). The waves are unidirectional, two dimensional, long-crested waves, and are generated by a wave maker whose
 380 paddles are driven by a total of 15 hydraulic pistons moving in the horizontal direction.

	Peak period	Significant wave height	Probability of occurrence in Hanstholm
Sea state 1	0.7407 s	0.0620 m	30%
Sea state 2	0.9259 s	0.0920 m	45%
Sea state 3	1.1111 s	0.1220 m	10%
Sea state 4	1.4815 s	0.1800 m	Extreme operation

Table 1: Sea state characteristics (with 1:20 scale ratio applied)

The wave moment estimation data are downsampled to 10 Hz, in order to reduce the computation burden of the prediction algorithms. The resulting

spectra are presented in Figure 6.

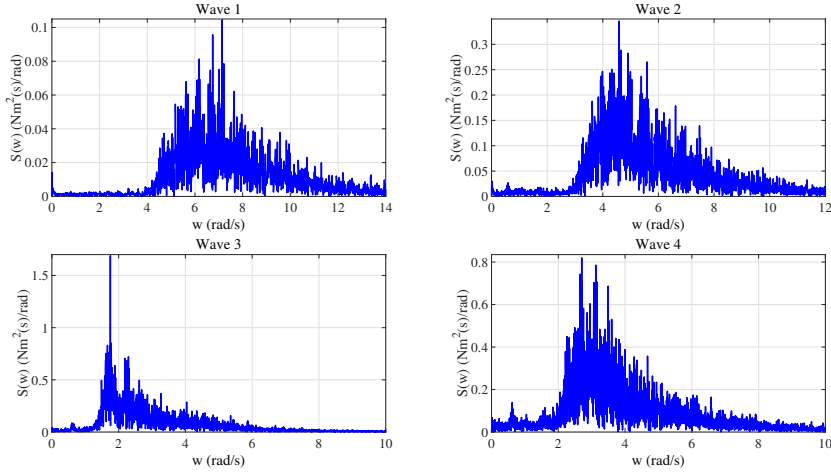


Figure 6: Wave spectra of sample data sets

385 **Remark 5:** The prediction performance corresponding to four time-invariant sea states is reported in this paper. Algorithm 1 and 2 have also been run, in real-time, with a time-varying sea state from sea state 2 to sea state 3, see [28] for more details.

5.2. Prediction performance

390 For a given prediction horizon N_p , the following performance index is used to determine the prediction accuracy, at time k ,

$$M_e(N_p) = \frac{\sum_{h=1}^{N_p} ((y(k+h) - \hat{y}(k+h|k)))^2}{M_y} \quad (35)$$

where M_y is the maximum of $y(k)$, $\forall k$. It is clear that the smaller $M_e(N_p)$, the better the forecasting model. A zero value for $M_e(N_p)$ implies that the wave time series is perfectly predicted over N_p steps into the future. Note that other
 395 indices such as mean square error, mean absolute error or mean absolute percentage error, etc, can also be used to measure the prediction accuracy [13], [19]. However they treat each horizon h separately, whereas the index 35 considers all the prediction horizons together.

5.3. Prediction results of the EKF approach

400 To obtain good results for the prediction, the order of the AR model (3) is an important factor. There is a trade-off between model complexity, which increases the computational burden to apply the EKF, and prediction performance. To guarantee a satisfactory performance, our experience shows that the order of the AR model should be greater or at least equal to $\frac{T_p}{T_s}$, where T_p is
 405 the maximum peak period of the considered sea states, and T_s is the sampling time. For example, for the 4 considered sea states, wave 4 has the largest peak period 1.4815(s). Since the sampling time is 0.1(s), the order of the AR model should be at least 15.

Table 2 shows, for wave 1, the trade-off between computation complexity
 410 and performance that led to the choice of $N_p = 32$. The computation time for $N_p = 20$, is taken as baseline.

Order	Increase in computation time	Prediction error \mathcal{E}
20	-	47.1166
26	12%	16.8177
32	28%	12.6587
40	54%	12.4838

Table 2: Trade-off between computational complexity and performance

The prediction error \mathcal{E} is computed as

$$\mathcal{E} = \sqrt{\sum_{k=1}^{N_d} \frac{(y(k + N_p) - \hat{y}(k + N_p|k))^2}{M_y}}$$

where N_d is the number of data, and M_y is the maximum of $y(k)$, $\forall k$.

Using Table 2, it can be observed that $N_p = 32$ is a good compromise
 415 between the performance and the computational complexity. Hence the order is set to be 32 for Algorithm 1.

Figure 7 presents the first four parameters a_1, a_2, a_3, a_4 for the four waves. It can be observed that the optimal parameters $\mathbf{a}(k)$ are time-varying. This

420 shows that the assumption that $\mathbf{a}(k)$ are constant is indeed restrictive. It is underlined that allowing $\mathbf{a}(k)$ to be time-varying is the way to cope with the fact that the sea state changes continuously, and that the AR model (3) is only an approximation of the real wave excitation force model.

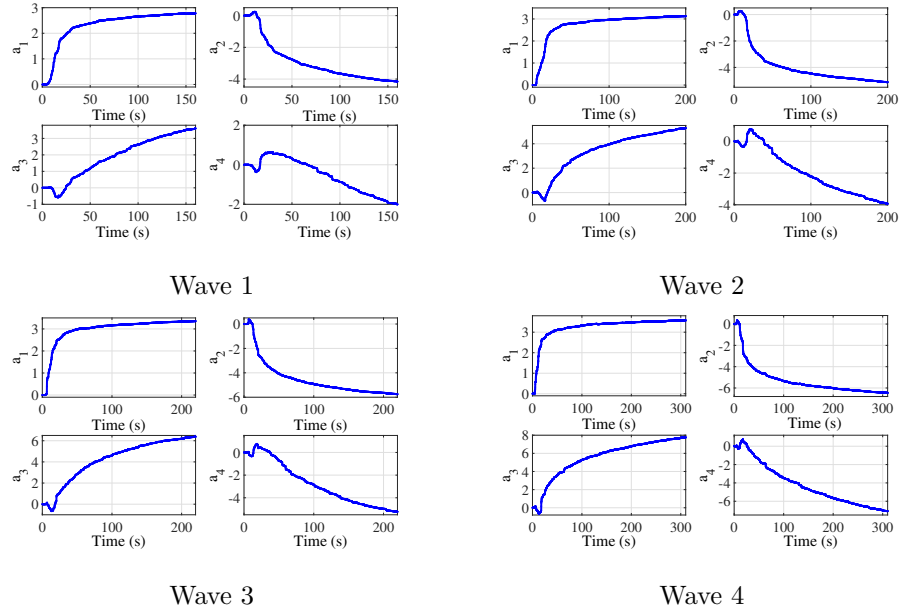


Figure 7: Optimal AR parameters. The time-varying nature of $\mathbf{a}(k)$ even for a time-invariant sea state is due to the fact that the AR model (3) is only an approximation of the exact model of the real system

425 Figure 8 shows the wave prediction performance of Algorithm 1. It can be observed that the predicted wave is in phase with the real wave. This feature is indeed very important for any WEC control algorithm.

Using the performance index (35), the prediction accuracies with $N_p = 10$ and $N_p = 20$ for algorithm 1 and the AR based approach via the minimization of a multi-step ahead cost function [13] are compared and shown in Figure 9. It can be observed that Algorithm 1 outperforms the mentioned solution.

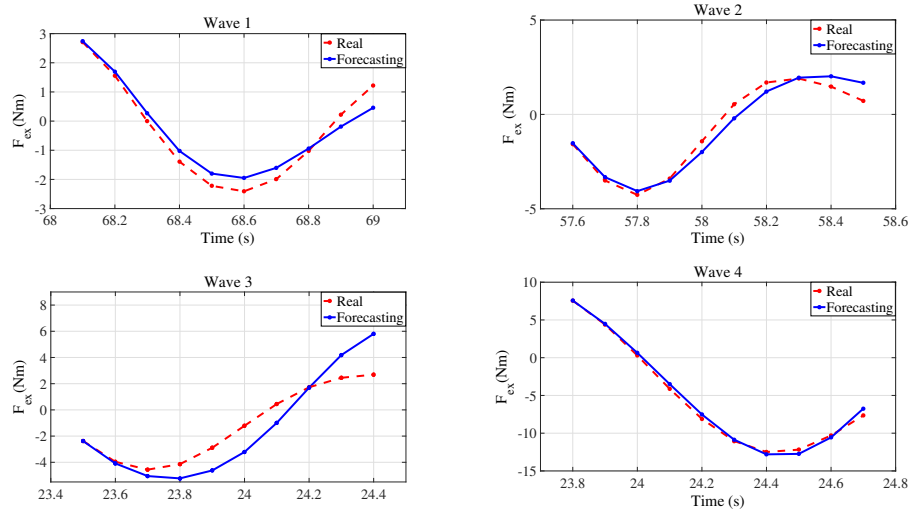


Figure 8: Wave prediction performance using Algorithm 1

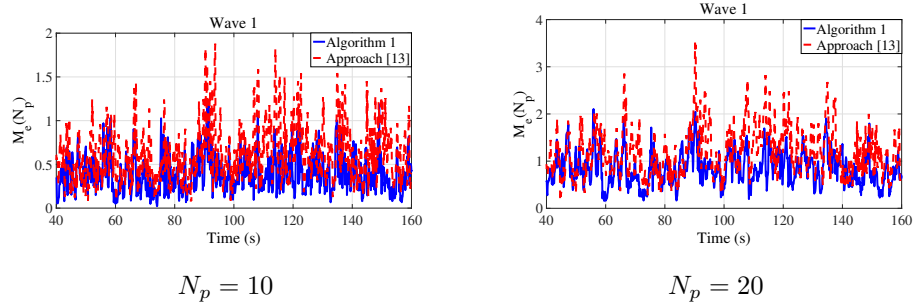


Figure 9: Prediction accuracy of Algorithm 1 and the approach in [13]

430 *5.4. Prediction results of the adaptive Kalman filter approach*

Since multiple models are used for algorithm 2, practice shows that it is enough to set the order of all the AR models to be 16. Figure 10 presents the wave prediction accuracy of Algorithm 2. It is clear that the algorithm yields good results.

435 Finally, using the normalized error index (35), the prediction accuracy with $N_p = 10$ for algorithm 1, and algorithm 2 are depicted in Fig. 11. Using the TIC/TOC function of Matlab 2015b, Table 3 shows the on-line computation

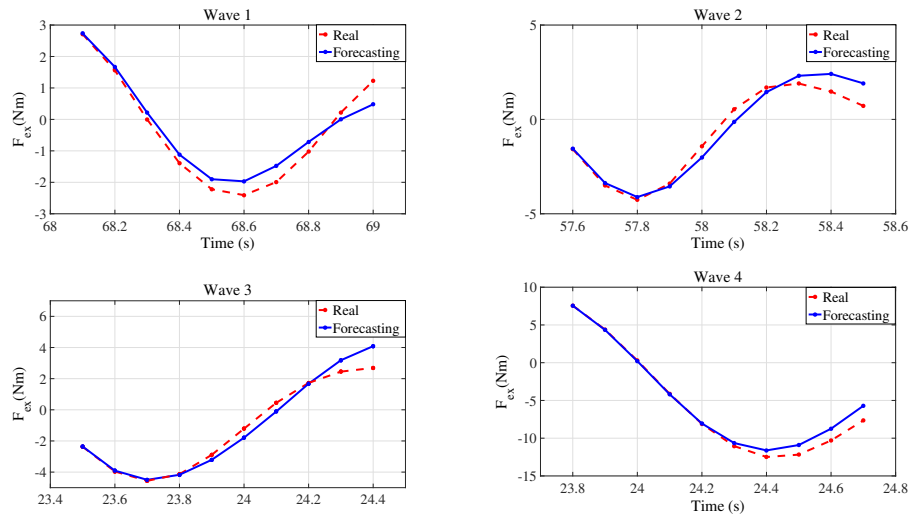


Figure 10: Wave prediction performance by using algorithm 2.

times for one discretization interval for algorithm 1 and algorithm 2. Looking at Fig. 11 and at Table 3, it is clear that there is a trade off between performance and computational complexity. It can be observed that algorithm 2 has the highest complexity. However it yields a better performance compared to algorithm 1, which has a more modest computational complexity.

	Online computation time (s)
Algorithm 1	0.0228
Algorithm 2	0.0312

Table 3: Duration (s) of online computations over one discretization interval for algorithm 1 and algorithm 2.

6. COMPUTATION OF INTERVAL FORECASTS

Until now, wave predictions have been expressed as scalars, which one will refer to as *point forecasts*, which do not give any idea about their likely accuracy. As a wave future value can be regarded as a random variable at the time the

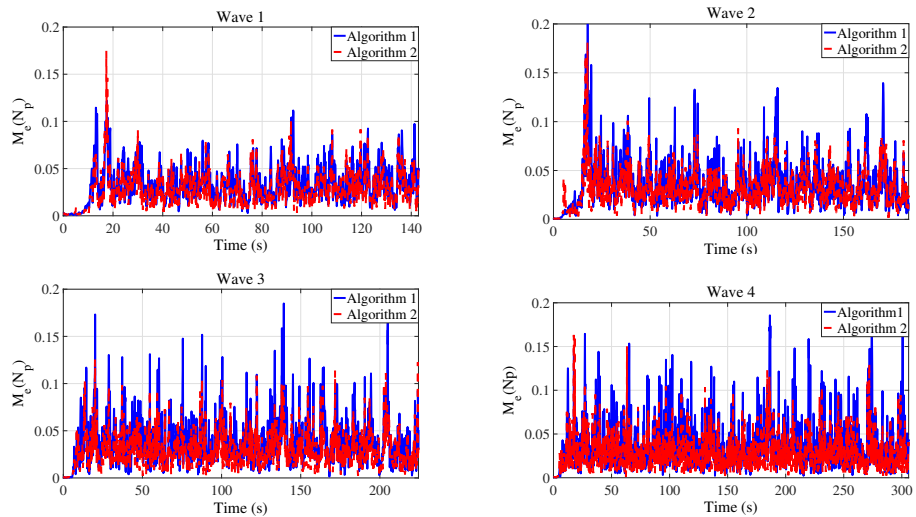


Figure 11: Prediction accuracy of algorithms 1 and 2.

forecast is made, it is more reasonable to express a wave forecast as a range of numbers, called an *interval forecast*. Providing point forecasts together with interval forecasts enables us to

- 450
- Assess future wave uncertainty.
 - Design different control strategies for the range of possible outcomes indicated by the interval forecasts.
 - Compare wave forecasts for different methods more precisely.
 - Investigate different scenarios using different assumptions in more detail.

455 Before proceeding further, one needs to define more rigorously what does mean by an interval forecast. An *interval forecast* consists of an upper and a lower limit between which a future value is expected to lie with a prescribed probability. The limits are called *prediction bounds* or *forecast limits*, while the interval is sometimes called a *prediction interval* [29], [30], [31].

460 Let us assume that the h -step ahead prediction error

$$\hat{e}(k+h|k) = y(k+h) - \hat{y}(k+h|k) \quad (36)$$

is zero-mean Gaussian with variance σ_h^2 . In the other words, the probability density function of $\hat{e}(k+h|k)$ is

$$p(\hat{e}(k+h|k)) = \frac{1}{\sqrt{2\pi}\sigma_h} \exp\left(-\frac{\hat{e}(k+h|k)^2}{2\sigma_h^2}\right) \quad (37)$$

In general, as the prediction horizon h is increased, the variance of the forecast error increases. In other words, the longer the lead time, the less
 465 accurate the forecast.

The probability that the error $\hat{e}(k+h|k)$ is contained within an interval $[-\delta, \delta]$ is calculated as follows,

$$P\{-\delta \leq \hat{e}(k+h|k) \leq \delta\} = \int_{-\delta}^{\delta} p(\mu) d\mu \quad (38)$$

Using (37), one obtains

$$P\{-\delta \leq \hat{e}(k+h|k) \leq \delta\} = \frac{1}{\sqrt{2\pi}\sigma_h} \int_{-\delta}^{\delta} \exp\left(-\frac{\mu^2}{2\sigma_h^2}\right) d\mu \quad (39)$$

The probability that the prediction error $\hat{e}(k+h|k)$ lies in the range $-\delta$ and
 470 δ with $\delta = n\sigma_h$, $n = 1, 2, 3, 4$ is given in Table 4.

n	$P\{-n\sigma_h \leq \hat{e}(k+h k) \leq n\sigma_h\}$
1	68.3%
2	95.5%
3	99.7%
4	99.9%

Table 4: Confidence intervals

Using Table 4, it is clear that the variance σ_h is all one needs to define the probability function of $\hat{e}(k+h|k)$ to lie in the interval $-n\sigma_h$ and $n\sigma_h$ with $n = 1, 2, 3, \dots$. Unfortunately, the exact value of σ_h is not directly available, since the wave is not known in the figure. One way to estimate σ_h , at time k ,
 475 is to use the past history of the prediction errors as,

$$\hat{\sigma}_h^2(k) = \frac{1}{k-1} \sum_{j=h+1}^k \hat{e}(j|j-h)^2 \quad (40)$$

Equation (40) uses *batch-processing* approach, which might be difficult to implement. An alternative way to estimate σ_h is to use the following recursive equation [32]

$$\hat{\sigma}_h^2(k) = \frac{k-2}{k-1} \hat{\sigma}_h^2(k-1) + \frac{1}{k-1} (y(k) - \hat{e}(k|k-h))^2 \quad (41)$$

Fig. 12, Fig. 13 present, respectively, the forecasting intervals (dash-dot green), the wave excitation moment prediction (solid blue), the real wave excitation moment (dashed red) for wave 1, wave 2, wave 3 and wave 4. These figures are obtained along with the 68.3% confidence interval. It is worth noticing that the forecasting intervals of algorithm 2 are generally smaller than the forecasting intervals of algorithm 1.

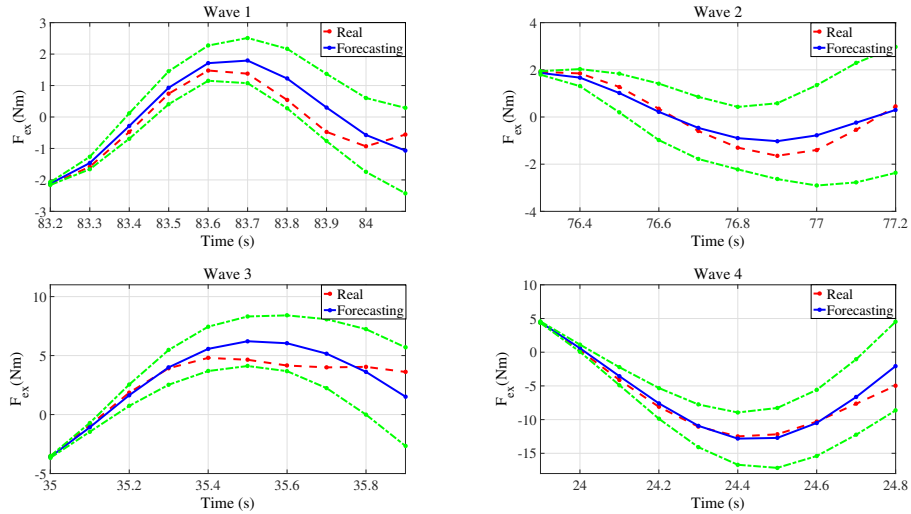


Figure 12: Forecasting intervals (dash-dot green), Wave excitation moment prediction (solid blue), Real wave excitation moment (dashed red) for algorithm 1.

485 7. CONCLUSION

The problem of short-term wave force forecasting was considered in the paper. Two new algorithms were proposed. For the set of data in this work, to improve the performance with respect to the one step ahead error minimization

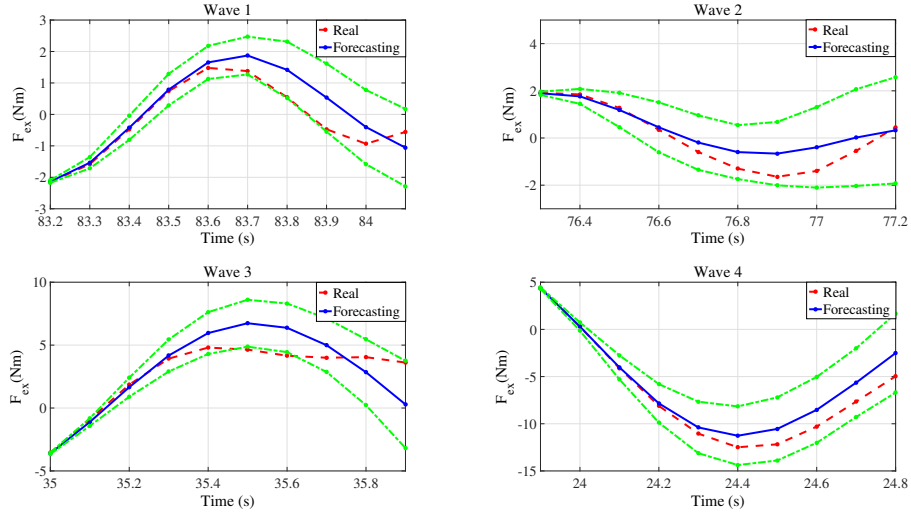


Figure 13: Forecasting intervals (dash-dot green), Wave excitation moment prediction (solid blue), Real wave excitation moment (dashed red) for algorithm 2.

cost function, a nonlinear multi-step ahead error minimization cost function is used for the first algorithm. It is shown that the criterion adopted in [13] is a limiting case when the sea state is assumed to be constant. An extended Kalman filter (EKF) is used to obtain a solution to the nonlinear optimization problem. The main advantage of the EKF is that it is recursive and hence is easy to implement.

The second algorithm illustrates how to avoid the error accumulation problem by adopting N_p separated models to forecast N_p steps ahead of the wave force. The solution is also in a recursive form, since a linear Kalman filter is used for each model. It is shown that the approach in [15] is a particular case, when the sea state is constant.

Together with the wave force estimation block and the control block, the two prediction algorithms were successfully implemented on a real WEC system [28].

References

- [1] J. Falnes, Optimum control of oscillation of wave-energy converters, *International Journal of Offshore and Polar Engineering* 12 (02).
- 505 [2] U. A. Korde, J. Ringwood, *Hydrodynamic Control Of Wave Energy Devices*, Cambridge University Press, 2016.
- [3] A. Babarit, A. Clément, Optimal latching control of a wave energy device in regular and irregular waves, *Applied Ocean Research* 28 (2) (2006) 77–91.
- [4] F. Saupe, J. Gilloteaux, P. Bozonnet, Y. Creff, P. Tona, Latching control
510 strategies for a heaving buoy wave energy generator in a random sea, in: *World Congress*, Vol. 19, 2014, pp. 7710–7716.
- [5] A. Babarit, M. Guglielmi, A. H. Clément, Declutching control of a wave energy converter, *Ocean Engineering* 36 (12) (2009) 1015–1024.
- [6] G. Li, M. R. Belmont, Model predictive control of sea wave energy
515 converters—part I: A convex approach for the case of a single device, *Renewable Energy* 69 (2014) 453–463.
- [7] H.-N. Nguyen, P. Tona, Wave excitation force estimation for wave energy converters of the point absorber type, *IEEE*, 2017.
- [8] J. Tedd, P. Frigaard, Short term wave forecasting, using digital filters, for
520 improved control of wave energy converters, in: *Proc. of Int. Offshore and Polar Eng. Conf*, Vol. 388, 2007, p. 394.
- [9] F. Serafino, C. Lugni, F. Soldovieri, A novel strategy for the surface current determination from marine x-band radar data, *IEEE Geoscience and Remote Sensing Letters* 7 (2) (2010) 231–235.
- 525 [10] F. Paparella, K. Monk, V. Winands, M. Lopes, D. Conley, J. V. Ringwood, Up-wave and autoregressive methods for short-term wave forecasting for an oscillating water column, *IEEE Transactions on Sustainable Energy* 6 (1) (2015) 171–178.

- [11] M. Belmont, J. Horwood, R. Thurley, J. Baker, Filters for linear sea-wave prediction, *Ocean Engineering* 33 (17) (2006) 2332–2351.
- [12] P. Frigaard, M. Brorsen, A time-domain method for separating incident and reflected irregular waves, *Coastal Engineering* 24 (3) (1995) 205–215.
- [13] F. Fusco, J. V. Ringwood, Short-term wave forecasting for real-time control of wave energy converters, *Sustainable Energy, IEEE Transactions on* 1 (2) (2010) 99–106.
- [14] P.-S. Yeraï, V. R. John, A critical comparison of AR and ARMA models for short-term wave forecasting, in: *Proceedings of the 12th European Wave and Tidal Energy Conference, EWTEC*, 2017.
- [15] B. Fischer, P. Kracht, S. Perez-Becker, Online-algorithm using adaptive filters for short-term wave prediction and its implementation, in: *Proceedings of the 4th International Conference on Ocean Energy (ICOE)*, Dublin, Ireland, 2012, pp. 17–19.
- [16] J. Hals, J. Falnes, T. Moan, Constrained optimal control of a heaving buoy wave-energy converter, *Journal of Offshore Mechanics and Arctic Engineering* 133 (1) (2011) 011401.
- [17] J. M. Jonkman, *Dynamics Modeling And Loads Analysis Of An Offshore Floating Wind Turbine*, ProQuest, 2007.
- [18] B. George, J. G. M., R. G. C., *Time Series Analysis: Forecasting And Control*, Pearson Education India, 1994.
- [19] L. Ljung, *System Identification: Theory For The User*, Springer, 1998.
- [20] D. Shook, C. Mohtadi, S. Shah, Identification for long-range predictive control, in: *IEE Proceedings D (Control Theory and Applications)*, Vol. 138, IET, 1991, pp. 75–84.

- [21] B. Wahlberg, L. Ljung, Design variables for bias distribution in transfer function estimation, *Automatic Control, IEEE Transactions on* 31 (2) (1986) 134–144.
- [22] R. Kashyap, Maximum likelihood identification of stochastic linear systems, *IEEE Transactions on Automatic Control* 15 (1) (1970) 25–34.
- [23] H.-N. Nguyen, F. Guillemin, On process noise covariance estimation, in: *Control and Automation (MED), 2017 25th Mediterranean Conference on,* IEEE, 2017, pp. 1345–1348.
- [24] P. R. Bélanger, Estimation of noise covariance matrices for a linear time-varying stochastic process, *Automatica* 10 (3) (1974) 267–275.
- [25] B. D. Anderson, J. B. Moore, *Optimal Filtering*, Courier Corporation, 2005.
- [26] K. J. Astrom, B. Wittenmark, *Adaptive Control*, Addison-Wesley Longman Publishing Co., Inc., 1994.
- [27] R. E. Kalman, A new approach to linear filtering and prediction problems, *Journal of Fluids Engineering* 82 (1) (1960) 35–45.
- [28] H.-N. Nguyen, G. Sabiron, P. Tona, M. M. Kramer, E. V. Sanchez, Experimental validation of a nonlinear MPC strategy for a wave energy converter prototype, in: *ASME 2016 35th International Conference on Ocean, Off-shore and Arctic Engineering*, American Society of Mechanical Engineers, 2016.
- [29] P. J. Brockwell, R. A. Davis, *Introduction To Time Series And Forecasting*, Vol. 1, Taylor & Francis, 2002.
- [30] W. William, S. Wei, *Time Series Analysis: Univariate And Multivariate Methods*, Addison Wesley, 1990.
- [31] B. Abraham, J. Ledolter, *Statistical Methods For Forecasting*, Vol. 234, John Wiley & Sons, 2009.

- ⁵⁸⁰ [32] R. Isermann, Fault-Diagnosis Systems: An Introduction From Fault Detection To Fault Tolerance, Springer Science & Business Media, 2006.